THE ANATOMICAL RECORD 294:1975–1990 (2011)

Morphological Correlates of the Grooming Claw in Distal Phalanges of Platyrrhines and Other Primates: A Preliminary Study

STEPHANIE MAIOLINO,[1]* DOUG M. BOYER,[2,3,4]
AND ALFRED ROSENBERGER[2,3,4]
[1]Interdepartmental Doctoral Program in Anthropological Sciences, Stony Brook University, Stony Brook, New York
[2]Department of Anthropology and Archaeology, Brooklyn College, City University of New York, Brooklyn, New York
[3]Department of Anthropology, City University of New York Graduate Center; New York Consortium in Evolutionary Primatology (NYCEP), New York, New York
[4]Department of Mammalogy, American Museum of Natural History, New York, New York

ABSTRACT

Grooming claws are present on the second pedal digits of strepsirhines and on the second and third pedal digits of tarsiers. However, their presence in New World monkeys is often overlooked. As such, the absence of a grooming claw is generally considered an anthropoid synapomorphy. This study utilizes a quantitative multivariate analysis to define grooming claw morphology and document its presence in platyrrhine monkeys. Our results show that owl monkeys possess grooming claws similar to those of strepsirhines, while titi monkeys possess grooming claw-like morphology. Therefore, we conclude that anthropoids are not clearly united by the absence of a grooming claw. Furthermore, due to their presence in three major primate clades, we infer that it is likely that a grooming claw was present on the second pedal digit of the ancestor of living primates. Therefore, we advise the reassessment of fossil adapids in light of the anatomical correlates described here. This should increase resolution on the homology and polarity of grooming claw morphology, and, therefore, will help provide a sharper picture of primate evolution. Anat Rec, 294:1975–1990, 2011. © 2011 Wiley Periodicals, Inc.

Key words: grooming claws; platyrrhines; distal phalanges; primate evolution; primate nails; tegulae

Most mammals possess keratinized digital end organs (e.g., claws, nails, hooves) on all or some of their digits. These structures are referred to as ungues (sing. unguis; adj. unguicular) regardless of the forms they take. Ungues are epidermally derived and composed primarily of dead, keratinized cells (Baden, 1970; Hildebrand and Goslow, 2001). Unguis form is largely related to the shape of the underlying distal phalanx (Clark, 1936; Hamrick, 2001, 2003). Specifically, the unguis wraps or folds over its dorsal, lateral, and medial sides (Bruhns, 1910; Clark, 1936; Homberger et al., 2009). In dorsoventral cross section, the unguis appears as an open curve; the degree to which the lateral and medial sides of this curve approximate one another varies among forms. Where the unguis projects distally beyond the fingertip, the space between the lateral and medial edges is filled

---

*Correspondence to: Stephanie Maiolino, Department of Anthropology, Stony Brook University, Stony Brook, NY 11794-4364. E-mail: smaiolin@ic.sunysb.edu

Received 15 September 2011; Accepted 16 September 2011
DOI 10.1002/ar.21498

Fig. 1. Unguis forms demonstrated in lateral (left) and dorsal (right) views. **A**: Falcula, third pedal digit of Sciurus sp. (SBU 2); **B**: Ungula, third pedal digit of Chlorocebus aethiops (SBU 5); **C**: Tegula, third pedal digit of *Saguinus fuscicollis* (SBU 16); **D**: Grooming claw, second pedal digit of *Lemur catta* (SBU 14).

to some degree with a cornified substance (Clark, 1936; Wake, 1992; Hildebrand and Goslow, 2001; Homberger et al., 2009). This substance is usually referred to as the subunguis, sole pad, sole horn, or sole plate. It is not clearly visible on many nail-bearing digits, but is present in a reduced form, often referred to as the hyponychium (Wake, 1992). Specifically, the hyponychium is a keratinous-like substance that forms a "plug" where the skin of the finger meets the undersurface of the nail (Zook, 2003).

Modern primates exhibit three unguicular forms: an ungula (pl. ungulae; adj. ungular) or nail, a claw-like tegula (pl. tegulae; adj. tegular), and a structure associated with grooming that is commonly referred to as a grooming or toilet claw. The claw-like ungues of nonprimate mammals are called falculae (sing. falcula; adj. falcular). Figure 1 provides examples of each unguis form. The principle anatomical differences associated with ungual form involve the shape of the unguis itself, the structure of its underlying phalanx, and the form and position of the digit's apical pad. Falculae (Fig. 1A) are longitudinally curved structures overlying dorsoventrally deep and mediolaterally narrow falcular phalanges (Clark, 1936; Hershkovitz, 1977; Spearman, 1985; Soligo and Müller, 1999; Hamrick, 2001). Falcular apical pads are positioned proximally and are often situated ventral to the distal interphalangeal joint (Rosenberger, 1977; Garber, 1980). Therefore, the shafts of falcular phalanges project distally beyond these pads. The two sides of a falcula extend below the ventral margin of the phalanx and therefore form a cleft or groove along phalanx's undersurface; subunguis fills most of this groove (Clark, 1936; Wake, 1992; Hildebrand and Goslow, 2001). Ungulae (Fig. 1B) are somewhat flattened structures which overlie dorsoventrally shallow and mediolaterally wide ungular phalanges (Clark, 1936; Hershkovitz, 1977; Spearman, 1985; Soligo and Müller, 1999; Hamrick, 2001). Ungular apical pads are enlarged and positioned more distally, ventral to the bodies of the ungular phalanges; ungular phalanges do not project far (or at all) beyond these apical pads (Bruhns, 1910). Subunguis runs between the apical pad and the undersurface of the ungula (Clark, 1936) but does not extend along the entire undersurface (Bruhns, 1910). Tegulae (Fig. 1C) are mediolaterally compressed ungues that are supported by dorsoventrally deep and mediolaterally narrow tegular phalanges (Clark, 1936; Hamrick, 1998). Differing from most falculae-bearing digits, the distal portions of tegular phalanges have flattened ventral borders (Clark, 1936). Tegular apical pads are well developed and positioned ventral to the bodies of tegular phalanges, though not for their entire length (Rosenberger, 1977; Garber, 1980). Subunguis fills much of the groove between the two sides of the tegula (Bruhns, 1910; Clark, 1936). These ungues are present on all manual digits and pedal digits II–V of callitrichine platyrrhines and on all manual digits and pedal digits III–V of the lemuriform strepsirhine *Daubentonia madagascariensis* (Clark, 1936; Hershkovitz, 1977; Rosenberger, 1977, 1979; Soligo and Müller, 1999). The second pedal digit of *Daubentonia* is described as bearing a grooming claw rather than a tegula (Soligo and Müller, 1999). Grooming claws (Fig. 1D; note that the digit in this photograph is in flexion at the distal interphalangeal joint) and their associated grooming phalanges appear similar to tegulae and falculae, but are mediolaterally wider, dorsoventrally deeper, and less pointed (Bluntschli, 1929; Soligo and Müller, 1999). Grooming apical pads are positioned ventral to the proximal portion of the body of the phalanx. Grooming phalanges project dorsally and at a steep angle (i.e., are dorsally canted), from the apical pads (Soligo and Müller, 1999). Subunguis fills much of the space between the two sides of the grooming claw (Bruhns, 1910; Clark, 1936). Grooming claws are present on the second pedal digits of strepsirhines and owl monkeys (*Aotus*; see more below) and on the second and third pedal digits of tarsiers (Bluntschli, 1929; Hershkovitz, 1977; Rosenberger, 1979; Fleagle, 1999; Soligo and Müller, 1999).

Historically, the term tegula was defined as a laterally compressed nail (Weber, 1928). In the literature (e.g., Hershkovitz, 1977), this term is sometimes used to represent an intermediate form between nails and claws; whereas the ungues of callitrichines are referred to as claws and the ungues of many platyrrhine monkeys (which are more laterally compressed than those of many catarrhines) are referred to as tegulae. In fact, there exists a continuum in distal phalanx shape between tegulae- and ungulae-bearing platyrrhines (Hamrick, 1998), while a form of claw-like ungulae are described in several strepsirhine species, e.g., *Euoticus elegantulus*, *Mirza coquereli*, and *Phaner furcifur* (e.g., Cartmill, 1972). The continuum and diversity of shape complicates the categorization of these features. For the sake of clarity and convenience, the term tegulae is here used to differentiate the claw-like primate ungues from the claws of nonprimates and solely refers to the extreme unguis morphology seen in callitrichine platyrrhines and *Daubentonia*.

Fossil and phylogenetic evidence strongly suggest that euprimate (extant primates and fossils associated with the two major clades, strepsirhines and haplorhines) ungulae are derived from mammalian falculae (Clark, 1936; Cartmill, 1974; Szalay and Dagosto, 1980; Spearman, 1985; Godinot and Beard, 1991). Historically, some researchers have suggested that primate characteristics, including ungulae, were the ancestral mammalian condition. These ancestral ungulae were modified into falculae during terrestrial phases in the evolutionary history of nonprimate mammals (Jones, 1916; Panzer, 1932). While most researchers today consider tegulae to be a derived form of primate ungulae (Pocock, 1917; Rosenberger, 1977; Ford, 1980; Garber, 1980; Martin, 1992; Hamrick, 1998; Soligo and Müller, 1999), some have argued that they are slightly modified falculae (Clark, 1936; Thorndike, 1968; Cartmill, 1974; Hershkovitz, 1977; Spearman, 1985). Similar controversy surrounds the grooming claw (Dagosto, 1990; Williams et al., 2010). To date, most arguments on whether the claw-like structures exhibited by primates (tegulae and grooming claws) should be considered derived or primitive have relied on unguis histology (Clark, 1936; Thorndike, 1968; Soligo and Müller, 1999). Initial studies of histology seemed to show distinctive differences between falculae and ungulae: Clark (1936) showed that falculae are comprised of two distinct layers, the superficial and deep strata, which are produced in different areas of the germinal matrix[1], the basal and terminal matrices, respectively. Ungulae were shown to possess only one layer, homologous to the superficial stratum. In contrast, the tegulae of callitrichines were shown to be comprised of two layers like falculae, but with a deep stratum that is reduced in thickness. Clark, therefore, interpreted tegulae to be slightly modified falculae. Subsequent studies have shown that the ungulae of some taxa (e.g., *Cebus*, *Lemur catta*, and some catarhines) are actually

---

[1] The germinal matrix is the germinal tissue which produces the

[1] The germinal matrix is the germinal tissue which produces the cells that become keratinized to form the unguis. This matrix is situated at the base, or root, of the unguis and lies deep to the eponychium (the fold of epidermis which covers the base of the unguis; in humans, this is the fold of skin from which the cuticle emerges).

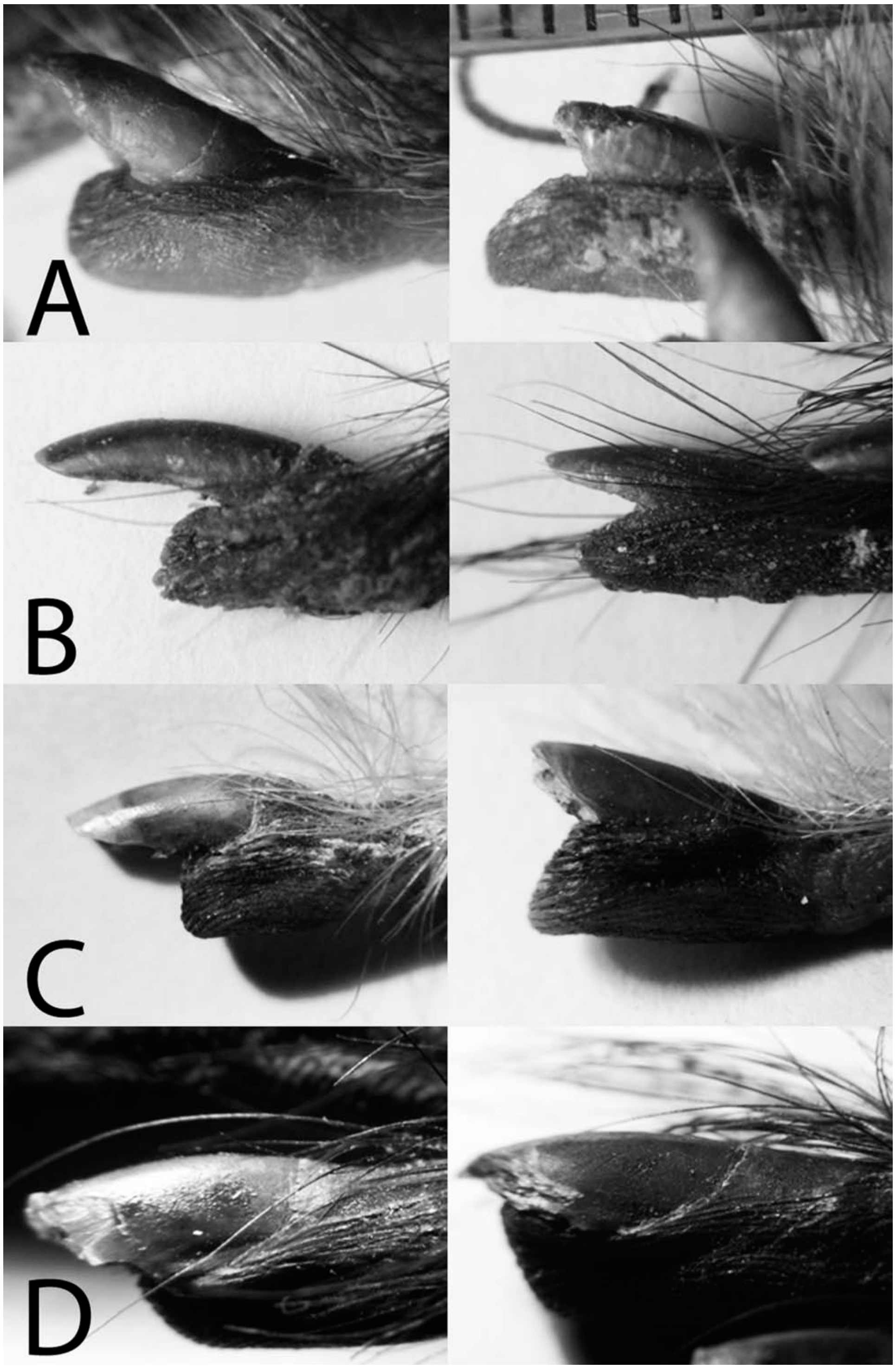

Fig. 2. Comparison of platyrrhine ungues on second (left) and third pedal digits (right). Photographs are taken from skins. **A**: *Aotus azarae* (AMNH 211478); **B**: *Callicebus muloch* (AMNH 211478); **C**: *Saimiri boliviensis* (AMNH 211615); **D**: *Cebus apella* (AMNH 98404).

comprised of two layers (Thorndike, 1968; Soligo and Müller, 1999), demonstrating that two layers are not unique to falculae and tegulae. Further, grooming claws are variable in their make-up as they may be comprised of one (*Microcebus* and *Galagoides*) or two (*Tarsius*) layers (Clark, 1936). These findings render histology ambiguous for determining the polarity of unguis-form.

Another argument for the derivation of grooming claws relies on assumptions of the functionalities of different unguis forms. Principally, Soligo and Müller

TABLE 1. Primate and non-primate sample used in this analysis

Species	Taxonomic Group	Unguis Form	Rays	Specimen Number
Didelphis sp.	Didelphidae (Didelphimorph)	Falcula	Third	SBU (3)
Phalanger orientalis	Phalangeridae (Diprotodont)	Falcula	Fourth	AMNH 79864
Tamandua sp.	Myrmecophagidae (Pilosan)	Falcula	Third	SBU (1)
Suricata suricatta	Herpestidae (Carnivoran)	Falcula	Third	AMNH 90441
Sciurus sp.	Sciuridae (Rodent)	Falcula	Third	SBU (2)
Galeopterus variegatus	Cynocephalidae (Dermopteran)	Falcula	Third	UNSM 15502
Tupaia glis	Tupaiidae (Scandentian)	Falcula	Third	AMNH 215175
Eulemur fulvus	Lemuridae (Strepsirhine)	Groom/Ungula	Second/third	SBU (13)
Hapalemur griseus	Lemuridae (Strepsirhine)	Groom/Ungula	Second/third	SBU (12)
Lemur catta	Lemuridae (Strepsirhine)	Groom/Ungula	Second/third	SBU (14)
Varecia variegata	Lemuridae (Strepsirhine)	Groom/Ungula	Second/third	AMNH 201384
Galago senegalensis	Galagidae (Strepsirhine)	Groom/Ungula	Second/third	SBU (15)
Nycticebus coucang	Lorisidae (Strepsirhine)	Groom/Ungula	Second/third	AMNH 16615
Tarsius bancanus	Tarsiidae (Tarsiiform)	Groom/Ungula	Second, third/fourth	AMNH 106754
Tarsius spectrum	Tarsiidae (Tarsiiform)	Groom/Ungula	Second, third/fourth	AMNH 109367
Ateles sp.	Atelinae (Platyrrhine)	Ungula	Second, third	SBU (10)
Brachyteles arachnoides	Atelinae (Platyrrhine)	Ungula	Second, third	AMNH 260
Pithecia pithecia	Pitheciinae (Platyrrhine)	Ungula	Second, third	SBU (8)
Callicebus cupreus	Callicebinae (Platyrrhine)	Groom/Ungula	Second/third	AMNH 130361
Aotus sp.	Aotinae (Platyrrhine)	Groom/Ungula	Second/third	SBU (11)
Cebus sp.	Cebinae (Platyrrhine)	Ungula	Second, third	SBU (7)
Saimiri sp.	Saimiriinae (Platyrrhine)	Ungula	Second, third	SBU (9)
Callithrix sp.	Callitrichinae (Platyrrhine)	Tegula	Third	AMNH 22994
Cebuella pygmaea	Callitrichinae (Platyrrhine)	Tegula	Third	AMNH 244101
Leontopithecus sp.	Callitrichinae (Platyrrhine)	Tegula	Third	AMNH 235275
Saguinus fuscicollis	Callitrichinae (Platyrrhine)	Tegula	Third	SBU (16)
Chlorocebus aethiops	Cercopithecini (Catarrhine)	Ungula	Second, third	SBU (5)
Macaca sp.	Papionini (Catarrhine)	Ungula	Second, third	SBU (4)
Hylobates sp.	Hylobatidae (Catarrhine)	Ungula	Second, third	SBU (6)

(1999) have argued that grooming claws must have been derived from a nail-like digit because they could not conceive of a selective pressure that would lead a population of already claw-bearing mammals to evolve a grooming claw. However, such an argument assumes that falculae are capable of playing the same role in grooming as do primate grooming claws. This may not be the case, as the claw-bearing diprotodont marsupials (including kangaroos and koalas) possess specialized syndactylus digits (second and third pedal rays) with distinctive ungues used in grooming (Jones, 1925; Goodrich, 1935). Subsequently, little is known about the potential pressures and conditions that would give rise to specialized grooming apparatus in some mammal groups.

On the other hand, the absence of a grooming claw is often considered an anthropoid synapomorphy. Thus, it has been used as evidence of phylogenetic affinities in fossil primates (Franzen et al., 2009). Nonetheless, the homologies, polarities, and tendencies for convergence of this trait are not well understood (Dagosto, 1990; Williams et al., 2010). Interpretations are further complicated as the distribution of grooming claws among primates is largely unappreciated. It was not until 1995 that the presence of a grooming claw was demonstrated in *Daubentonia* (Soligo, 1995; Soligo and Müller, 1999), evinced by the dorsally canted unguis and shape of the second pedal digit in comparison to the remaining lateral digits. The presence of grooming claws in owl monkeys was reported by Bluntschli in 1929 but has subsequently been mentioned in only a handful of other works (Hill, 1960; Rosenberger, 1979; Fleagle, 1999). Bluntschli also reported grooming claws in wild caught *Saimiri* and *Pithecia* but noted variation within species and was unable to identify these features in zoo specimens. Additionally, visual inspection of primate skins held in the mammalogy collection of the American Museum of Natural History suggests the presence of a grooming claw in *Callicebus* and a range of variation in the form of the second pedal digits of other platyrrhine species (Fig. 2). Clearly, a better understanding of the presence and morphological variation of grooming claws within platyrrhine monkeys is needed to better interpret the phylogenetic significance of this trait.

The research presented here quantitatively defines unguis forms (ungulae, tegulae, grooming claws, and nonprimate falculae) based on distal phalanx morphology. Distal phalanges are used with the hope that these analyses will ultimately be applicable to the fossil record. Quantitative analyses assess the distribution of platyrrhine-like grooming claws among extant primates, compare them to those of tarsiers and strepsirhines, and compare tegulae to other unguis forms. Qualitative observations of discrete traits are also made and the usefulness of these features in addressing the polarity of unguis form is discussed.

MATERIALS AND METHODS

Materials

Distal phalanges from one individual of 22 primate and seven nonprimate mammalian species (Table 1) were digitally photographed or microCT scanned. Falcular phalanges were sampled from third pedal digits of nonprimate mammals, with the sole exception of *Phalanger orientalis*. *P. orientalis* is a diprotodontid marsupial and as such possesses syndactylus second and third pedal digits. The morphology of the syndactylus digits is atypical of the remaining digits and, therefore, the

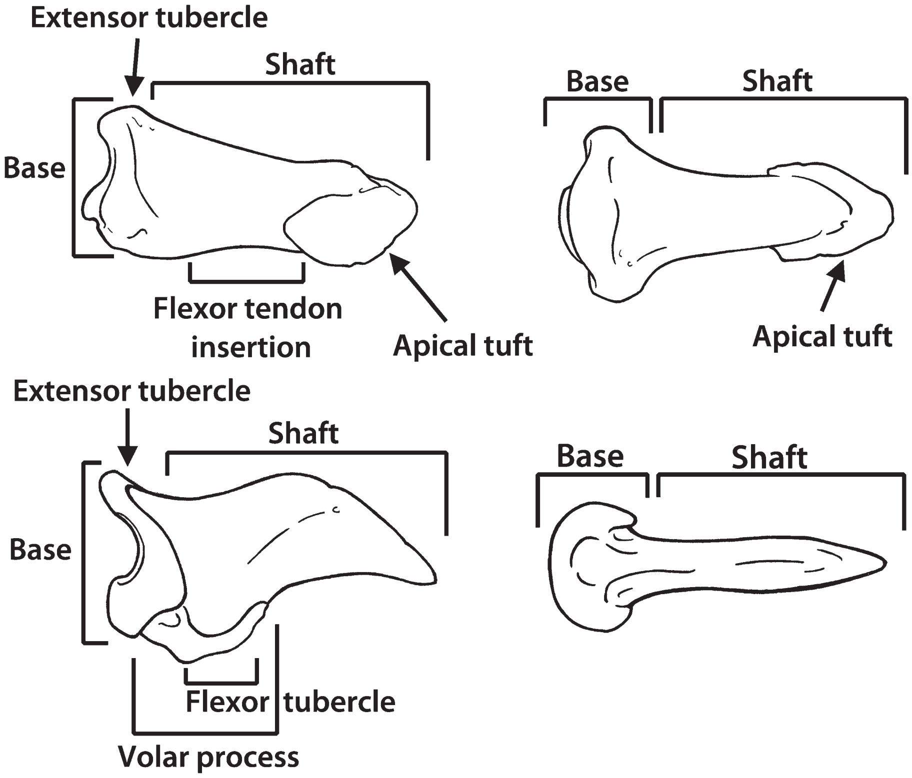

Fig. 3. Anatomical features referenced in this analysis. Above: ungular phalanx; Below: falcular phalanx; Left: lateral views; Right: dorsal views.

fourth pedal digit was used instead. To avoid potential phylogenetic and functional bias, phalanges of both arboreal and terrestrial mammals from a wide range of orders (carnivorans, rodents, marsupials, and euarchontans) were included. Tegular phalanges were sampled from the third pedal digits of callitrichine platyrrhines, while grooming phalanges were sampled from the second pedal digits of strepsirhine primates and the second and third pedal digits of tarsier species. Ungular phalanges were sampled from the second, third and, in the case of tarsiers, the fourth pedal digits. The inclusion of both second and third pedal digits allows for comparisons between grooming phalanges and second pedal ungular phalanges of different species, comparisons between grooming phalanges and ungular phalanges of the same species, and between third pedal digits of different unguis forms. All materials used in this analysis are housed at the American Museum of Natural History (AMNH), the University of Nebraska Science Museum (UNSM), and Stony Brook University (SBU). The SBU specimens in this analysis are not associated with specimen numbers and are therefore given provisional numbers for ease of reference within this article. Provisional numbers are presented in parentheses.

Data were collected from each specimen in one of two ways: digital photography or microCT scanning. All AMNH specimens, with the exception of the two tarsiers, were digitally photographed in two views, dorsal and lateral. Specimens were carefully oriented according to the long axis of the phalanx and a ruler was placed near each specimen as a scale. All SBU specimens are wet specimens preserved in a formalin solution. Individual digits of these specimens were scanned with a VivaCT75 MicroCT scanner at Stony Brook University at a resolution of 39 μm. Surface reconstructions from the resulting DICOM files were generated using Amira 5.2.0. Separate surfaces were generated for soft tissue and bone through utilization of a masking function available within the Labelfield module. Such reconstructions allow for the easy visualization of the relationship between soft tissue and bone within the digit tips. The tarsier distal phalanges (AMNH 106754 and 109367) and the distal phalanges of the colugo (UNSM 15502) are preserved within the feet of dry skins. To nondestructively access these, the skins were also scanned at SBU at a resolution of 20.5 and 30 μm, respectively. Reconstructions of these phalanges were generated in the same manner as for those contained within wet specimens. Note that soft tissue was not reconstructed from dried skin specimens. Finally, for all microCT scans, snapshots of surface reconstructions aligned in dorsal and lateral views were generated using Amira.

Figure 3 depicts anatomical features referenced in this article. The flexor and extensor tubercles are the attachment sites for the long digital flexor and extensor tendons. The flexor tendon insertion of the ungular phalanx is less distinct in lateral view than that of the falcular phalanx; the general area of its insertion is indicated in Fig. 3. The volar process of the falcular phalanx contains the flexor tubercle but is also associated with the apical pad. The base corresponds to the proximal epiphysis and contains the articular facet. See Homberger et al. (2009), Shrewsbury et al. (2003), and Mittra et al. (2007) for

TABLE 2. Descriptions of measurements taken on each distal phalanx

Names (Abbreviation)	Descriptions	View
Base height (BH)	Maximum height of base (⊥ to PDA)	Lateral
Base width (BW)	Maximum width of base (∥ to MLA)	Dorsal
Total phalanx length (TPL)	Total length of distal phalanx (∥ to PDA)	Lateral
Shaft height at 1/4 length (SH-1/4)	Height of shaft taken at 1/4 of the length of the shaft (⊥ to PDA)	Lateral
Shaft width at 1/4 length (SW-1/4)	Width of shaft taken at 1/4 of the length of the shaft (⊥ to PDA)	Dorsal
Shaft height at 3/4 length (SH-3/4)	Height of shaft taken at 3/4 of the length of the shaft (⊥ to PDA)	Lateral
Shaft width at 3/4 length (SW-3/4)	Width of shaft taken at 3/4 of the length of the shaft (⊥ to PDA)	Dorsal
Facet shaft angle (FSA)	Angle between PDA and articular facet	Lateral
Volar feature length (VFL)	Length of volar process or volar surface (∥ to PDA)	Lateral

View refers to the orientation of the phalanx as the measurement is taken.
Abbreviations: PDA, Proximodistal axis of phalanx; MLA, Mediolateral axis of phalanx.

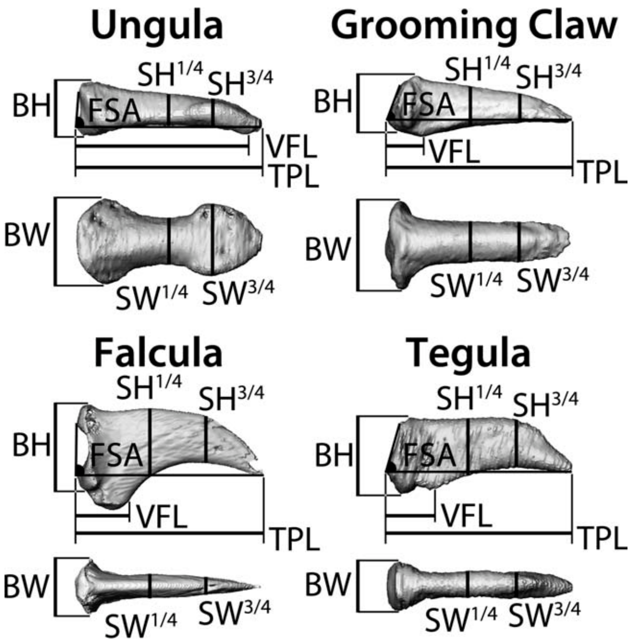

Fig. 4. Measurements used in this analysis demonstrated on ungular [*Tarsius spectrum* (AMNH 109367), fourth pedal digit], falcular [*Sciurus sp.* (SBU 2), third pedal digit], grooming claw-bearing [*Eulemur fulvus*, (SBU 13) second pedal digit], and tegular [*Saguinus fuscicollis* (SBU 16), third pedal digit] distal phalanges. Lateral views are situated above dorsal views.

detailed descriptions of the anatomical features of distal phalanges.

Methods

A set of nine measurements were taken from digital photographs or snapshots of microCT reconstructions using SigmaScan Pro 5.0 (Table 2; Fig. 4). Measurements were taken in relation to two principal axes of the distal phalanx, the proximodistal axis and the mediolateral axis. The proximodistal axis is the long axis of the phalanx and is defined as the axis which passes through the inferior margin of the articular facet and the distalmost tip of the phalanx. The mediolateral axis is perpendicular to the proximodistal axis in the mediolateral plane. The positions at 1/4 and 3/4 of the shaft were located relative to the proximodistal length of the shaft. The measurement, facet-shaft angle (FSA), is the angle between the long axis of the phalanx and a line which passes through the superior and inferior margins of the articular facet. This angle represents the degree to which the shaft is canted in relationship to the orientation of the base. Volar feature length (VFL) refers to the portion of the distal phalanx which is surrounded by the apical pad (Fig. 5); the position and extent of this structure varies among phalanx forms. For falcular phalanges, this is the volar process (Fig. 3); it is a distinct expanded structure on the volar surface of the proximal portion of the phalanx. In ungular phalanges, this is the contoured volar surface (Fig. 5: red line) of the phalanx which ends in an angle with a portion of the phalanx which faces more distally (Fig. 5: blue line). In falcular and ungular phalanges, the extent of the volar feature demarcates two portions of the phalanx: one that is surrounded by the apical pad and one which underlies the unguis, thus projecting upward or distally beyond the margins of the apical pad. Tegular and grooming phalanges possess volar features that resemble the volar processes of falcular phalanges. However, the differ as they are not as closely associated with the junction between the two aforementioned portions of the phalanx.

Nonangular measurements were converted into size-adjusted shape variables through division by the geometric mean (Jungers et al., 1995). Variables are normally distributed, verified using 1-sample Kolmogorov–Smirnov tests ($P > 0.05$). However, when data are grouped according to unguis forms, many variables lack homogeneity of variance (Levene's tests, $P < 0.01$). Data were analyzed using a principal components analysis (PCA) of a correlation matrix and nonparametric multivariate analysis of variance (npMANOVA) based on correlation as a measure of distance with posthoc pairwise npMANOVAs in Past v2.03 (Hammer et al., 2001), Kruskall–Wallis tests with posthoc pairwise Tamhane's T2 tests and boxplots in SPSS v17.0, and *t* tests calculated in Microsoft excel. Tamhane's T2 tests were chosen as they do not require equal variances. The significance level of these tests is assessed using a *P* value of 0.01. In addition to the analysis of quantitative traits, careful

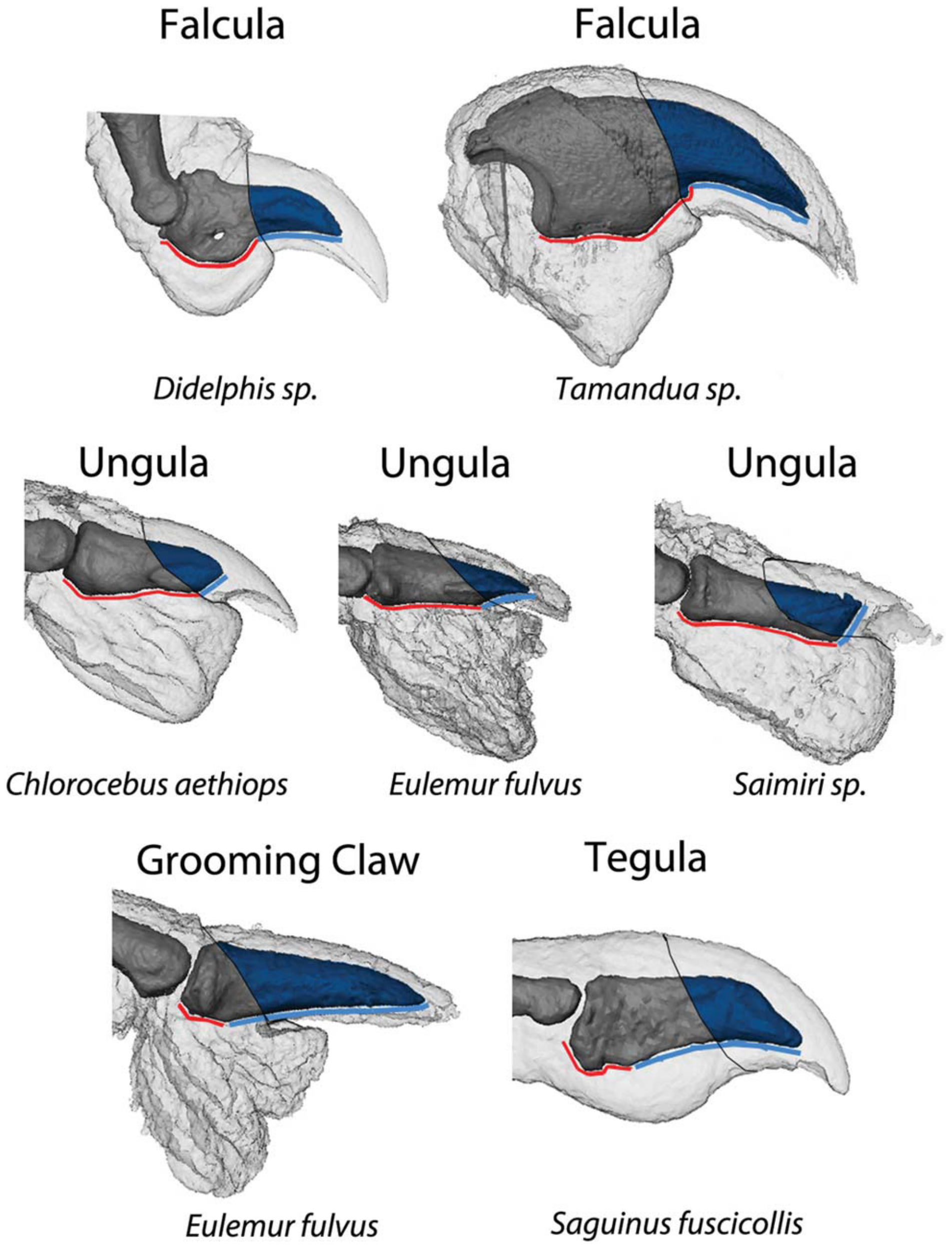

Fig. 5. Images from MicroCT scans of wet specimens. The soft tissue is rendered transparent to show the underlying bone. Volar features are outlined in red. Portions of phalanges, which are surrounded only by keratinous structures and associated tissue, are colored in blue. The junctions between keratinous structures and the rest of the digit are outlined in black as they are not well distinguished when soft tissue is rendered transparent. The locations of the outlines are obtained by changing the soft tissue to "shaded."

visual assessment of discrete traits is used in an attempt to identify possibly homologies among unguis forms.

RESULTS

The first two components of the PCA account for 71.3% of the variance. PC1 has an eigenvalue of 4.9 and explains 54.5% of the variance, while PC2 has an eigenvalue of 1.5 and explains 16.8% (Fig. 6). See Table 3 for component loadings reported as Pearson correlation coefficients. PC1 separates ungular phalanges from falcular and tegular phalanges. By comparison, ungular phalanges are shorter, have wider and shallower bases and shafts, and longer volar features. Falcular and tegular phalanges are not distinguished from one another. PC2 separates grooming phalanges from other forms. Grooming phalanges have lower facet shaft angles and shorter volar features than ungular phalanges. The second pedal digit of *Aotus* plots most closely to the grooming claws of strepsirhines and tarsiers, while that of *Callicebus* plots between grooming and ungular phalanges. The second pedal digits of other noncallitrichine platyrrhine species plot within or very close to ungular phalanx space.

The npMANOVA shows that there are significant differences among distal phalanges of different unguis forms ($P < 0.0001$). Note that the second pedal digits of platyrrhines have been excluded from this analysis. Posthoc comparisons show significant differences for all pairwise comparisons ($P < 0.003$).

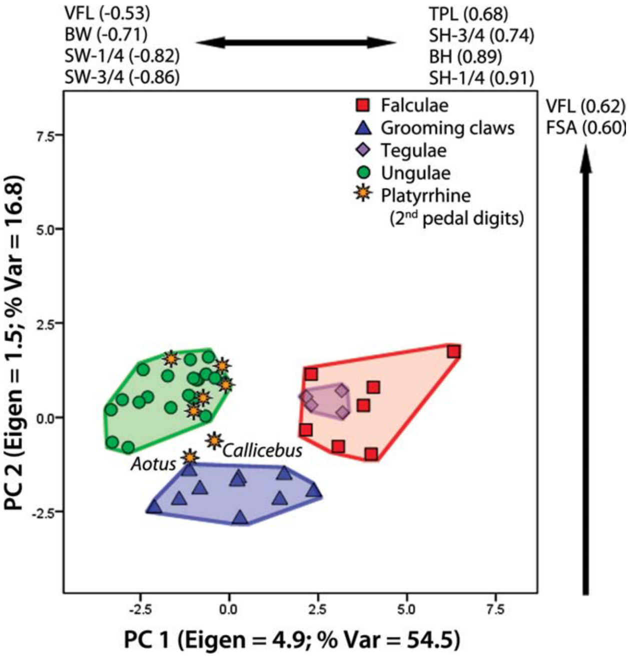

Fig. 6. Bivariate plot of the first two principal components from the PCA.

TABLE 3. The loadings of each component reported as Pearson correlation coefficients

Variables	PC1	PC2
BH	0.89	–0.30*
BW	–0.71	–0.43
TPL	0.68	–0.49
SH-1/4	0.91	–0.08*
SW-1/4	–0.82	–0.18*
SH-3/4	0.74	0.47
SW-3/4	–0.86	–0.03*
FSA	0.30*	0.60
VFL	–0.53	0.62

*Insignificant correlation ($P > 0.01$).

A series of Kruskal–Wallis tests show that there are significant differences among distal phalanges of different unguis forms for all variables ($P < 0.001$); again, the second pedal digits of platyrrhines have been excluded from this analysis. Table 4 presents the results of posthoc pairwise Tamhane's T2 tests. The results of t tests comparing the second pedal digits of *Aotus* and *Callicebus* values to unguis group means show that the grooming claw of *Aotus* is significantly different from the falculae group for the variables BH and SW-3/4, from the tegulae group for BH and SW-1/4, from the ungulae group for VFL, but not from the grooming claw group. *Callicebus* is significantly different from the tegulae group for TPL, SH-3/4, BW, SW-1/4, from the ungulae group for SH-1/4 and VFL, but not from the falculae or grooming claw groups. Significant P values for these comparisons are considered less than 0.01, and it should be noted that the second pedal phalanges of platyrrhines were excluded from the computations of group means. Table 5 presents group means and standard deviations for each group and individual values for the platyrrhine second pedal digits; the latter are excluded from the means of other groups. Figure 7 shows boxplots depicting group ranges, and Table 6 describes group morphologies.

Among platyrrhines, the second pedal digits of *Aotus* and *Callicebus* are most similar to the grooming claws of other primate taxa. The *Aotus* phalanx shares the characteristic trait of being more dorsally canted with a shorter volar feature than ungulae-bearing phalanges. Accordingly, its value for FSA (63.3) is outside the range of values for ungulae (lowest value is 66.7), but is not significantly different. The *Callicebus* phalanx shares the characteristic traits of a shorter volar feature and a more strongly tapering shaft than ungulae-bearing phalanges, but is not strongly dorsally canted (FSA = 85.5) and is even slightly less so than its third pedal digit (FSA = 80.5). This result seems odd as observations on primate skins show that this structure appears to have a stronger dorsal cant than that of the third pedal digit (Fig. 2B). Therefore, a better understanding of within species (and within genus) variation is necessary to interpret the morphology of *Callicebus*. The second pedal digits of other platyrrhines are not at all distinguished from ungular digits when considered in a multivariate context. However, it is relevant to observe that second

TABLE 4. The results of post hoc pairwise Tamhane's T2 tests comparing unguis form groups

	FxG	FxT	FxU	GxT	GxU	TxU
BH	ns	ns	$P < 0.001$	ns	ns	ns
BW	$P < 0.004$	ns	$P < 0.006$	$P < 0.001$	ns	$P < 0.001$
TPL	ns	ns	$P < 0.001$	ns	$P < 0.001$	$P < 0.001$
SH-1/4	$P < 0.006$	ns	$P < 0.001$	ns	ns	$P < 0.001$
SW-1/4	ns	ns	ns	$P < 0.01$	ns	$P < 0.001$
SH-3/4	ns	ns	ns	$P < 0.001$	ns	$P < 0.001$
SW-3/4	$P < 0.001$	ns	$P < 0.001$	ns	ns	$P < 0.003$
FSA	ns	ns	ns	$P < 0.001$	$P < 0.001$	ns
VFL	ns	$P < 0.006$	$P < 0.001$	ns	$P < 0.001$	ns

Comparisons are considered significant at a P value of 0.01.
Abbreviations: F, Falculae group; G, Grooming claw group; T, Tegulae group; U, Ungulae group.

TABLE 5. Variable group means and standard deviations (in parentheses) for unguis form groups and individual values for all platyrrhine second pedal digits

	BH	BW	TPL	SH-1/4	SW-1/4	SH-3/4	SW-3/4	FSA	VFL
Falculae	1.60 (0.15)	1.01 (0.14)	3.23 (0.24)	1.44 (0.27)	0.49 (0.14)	0.87 (0.30)	0.36 (0.08)	92.88 (17.64)	1.00 (0.18)
Groom	1.28 (0.31)	1.32 (0.16)	3.35 (0.35)	0.92 (0.21)	0.66 (0.15)	0.43 (0.07)	0.60 (0.12)	61.80 (4.70)	1.24 (0.15)
Tegulae	1.38 (0.17)	0.88 (0.02)	3.38 (0.12)	1.18 (0.08)	0.47 (0.02)	0.75 (0.04)	0.36 (0.10)	77.64 (3.77)	1.70 (0.20)
Ungulae	0.91 (0.08)	1.30 (0.23)	2.49 (0.29)	0.68 (0.09)	0.71 (0.10)	0.54 (0.10)	0.71 (0.16)	77.79 (6.48)	2.04 (0.32)
Aotus	0.99	1.22	2.81	0.79	0.76	0.54	0.82	63.30	1.11
Callicebus	1.09	1.46	2.58	1.06	0.73	0.48	0.60	85.51	1.08
Pithecia	0.81	1.20	2.84	0.79	0.78	0.56	0.58	73.60	1.79
Brachyteles	1.05	1.19	3.05	0.65	0.47	0.59	0.51	76.83	2.87
Ateles	0.70	1.17	2.46	0.70	0.78	0.61	0.66	83.50	2.25
Cebus	0.95	1.04	2.99	0.68	0.60	0.51	0.70	66.70	2.33
Saimiri	0.96	1.05	2.72	0.73	0.59	0.73	0.60	69.50	1.91

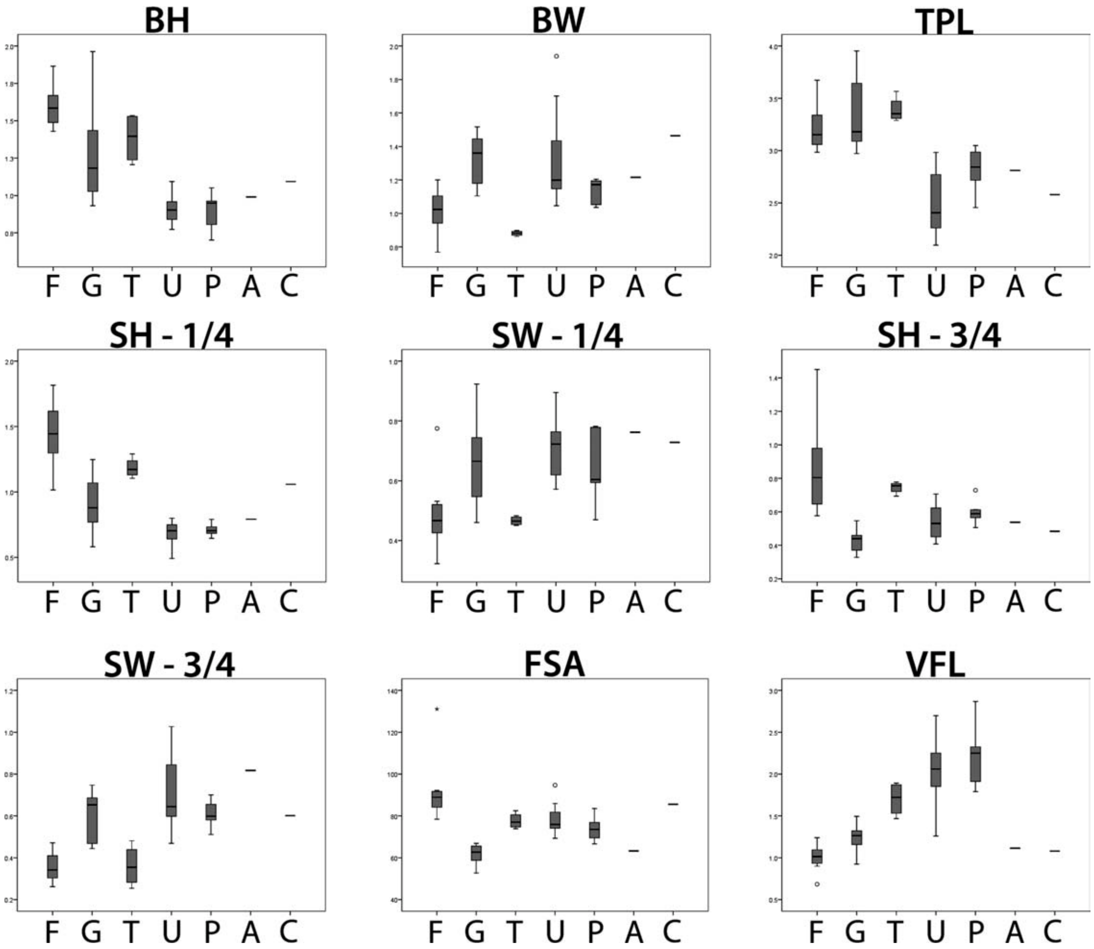

Fig. 7. Boxplots depicting group ranges for each variable. Abbreviations: F, Falculae phalanges; G, Grooming phalanges; T, tegular phalanges; U, ungular phalanges; P, second pedal digits of platyrrhines (excludes *Aotus*, *Callicebus*, and *Saguinus*); A, second pedal digit of *Aotus*; C, second pedal digit of *Callicebus*.

TABLE 6. Morphological descriptions of unguis forms and the second pedal digits of *Aotus* and *Callicebus*

	Length	Base	Shaft	Volar feature	Cant
Falcule	Long	Deep and narrow	Deep and narrow	Short	Straight to dorsal
Groom	Long	Deep and wide	Shallow, wide, tapers distally	Short	Strongly ventral
Tegulae	Long	Deep and narrow	Deep and narrow	Intermediate	Straight to slightly ventral
Ungulae	Short	Shallow and wide	Shallow and wide	Long	Straight to slightly ventral
Aotus	Short	Shallow and wide	Shallow and wide	Short	Ventral
Callicebus	Short	Shallow and wide	Shallow, wide, tapers distally	Short	Straight

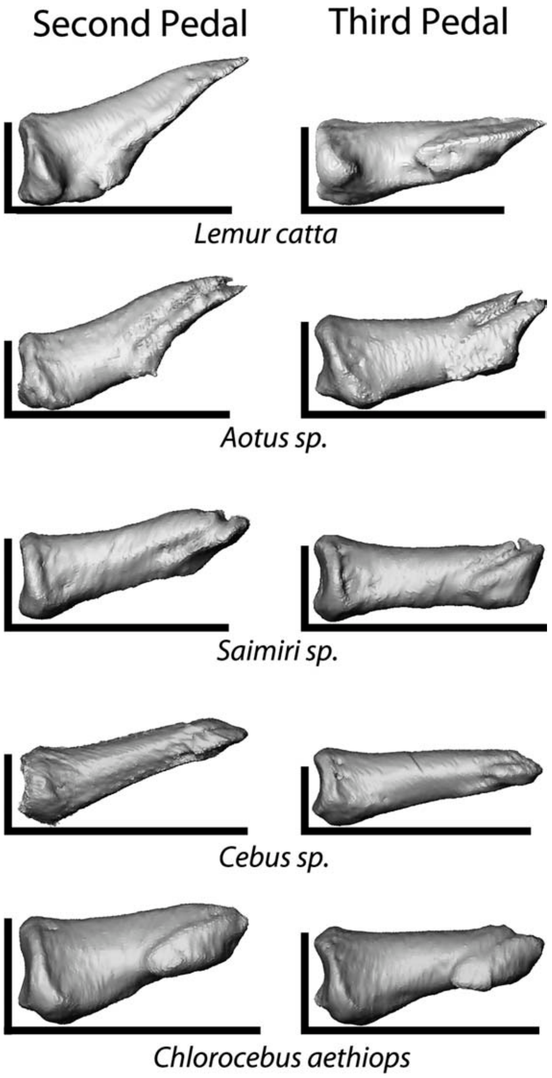

Fig. 8. Comparisons of ventral cant of second and third pedal digits. All digits have been scaled to a similar length.

pedal digits of several species are more strongly canted than the corresponding third in *Brachyteles arachnoides* (76.8 vs. 83.2), *Cebus sp.* (66.7, 78.9), *Saimiri sp.* (69.5, 76.1), and to a lesser degree *Pithecia pithecia* (73.6, 79.8) (Fig. 8). An increased dorsal cant can also be observed in the second pedal digits of the catarrhine *Chlorocebus aethiops* (69.3, 74.5) and *Macaca sp.* (74.6, 84.2). Again, an understanding of the variation within species is needed to better interpret the significance of such results.

Finally, a qualitative assessment reveals that primate ungular, tegular, and grooming phalanges are united by the presence of apical tufts, which are absent in falcular phalanges. While the extent and shape of this feature is highly variable, this trait appears to link all extant primate distal phalanges (Fig. 9). Primate apical tufts are thought to be associated with the stability and support of the apical pad; numerous fibrous bands which anchor the apical pad to the ventral surface of the apical tuft have been documented in humans (Shrewsbury et al., 2003; Mittra et al., 2007). In tegular and grooming phalanges, the apical tuft is positioned distally to the apical pad and thus cannot act to anchor it. If the function of the apical tuft is to anchor and support the apical pad, it is surprising to observe this feature on distal phalanges in which it is not in contact with the apical pad.

DISCUSSION

The Apical Tuft

The presence of an apical tuft appears to distinguish primate distal phalanges from nonprimate falcular phalanges. Like ungular and unlike falcular phalanges, tegular and grooming phalanges possess apical tufts (although somewhat reduced). Their presence in nonungular forms has not been previously documented. However, Clark (1936) did note that the ventral surfaces of the distal portions of primate tegular phalanges are flattened. It seems likely that this reflects the presence of a rudimentary apical tuft. Regardless, the presence of an apical tuft on the distal portion of the phalanx seems to unite all living primates to the exclusion of other mammalian groups.

Ungulae

Two other qualitative features have been associated with primate phalanges to the exclusion of nonprimate phalanges: absence of a distinct extensor tubercle and the lack of a sesamoid bone at the ventral aspect of the distal interphalangeal joint (Clark, 1936; Garber, 1980). The extensor tubercle does not appear to be a consistent difference between primates and nonprimates. Many falcular phalanges of nonprimate mammals lack a distinct extensor tubercle; these include pteropodid bats, some pilosans, and even the fossil plesiadapid plesiadapiforms (SM, Pers. Obs.; Bloch and Boyer, 2007). Further, there seems to be variation in the extent of the extensor tubercle within primate ungular phalanges (Fig. 9: compare *L. catta* to *G. senegalensis*). Additionally, most falcular phalanges appear to be associated with well-developed distal interphalangeal sesamoids while lateral ungular phalanges lack them. However, it should be noted that pollices and halluces of most primates are associated with well-developed sesamoids (SM, Pers. Obs.; Shrewsbury et al., 2003). Because of high levels of variation among digits, it seems that the most consistent differences between ungular and falcular phalanges are the presence of an apical tuft in ungulars, relative dorsoventral height and mediolateral width, and the relative length of the portion of the phalanx (volar process of falculars, contoured volar surface of ungulars) which is associated with apical pad.

Tegulae

Tegular and falcular phalanges are not well distinguished in this multivariate context. Of the variables considered within this analysis, the most pronounced difference between them is that tegular phalanges tend to possess relatively longer volar features than do falculars (Table 4, VFL; Fig. 7, VFL). This seems to indicate that the apical pad extends further distally along the shaft of the phalanx in tegular digits. Apical pad position has previously been suggested to differ between

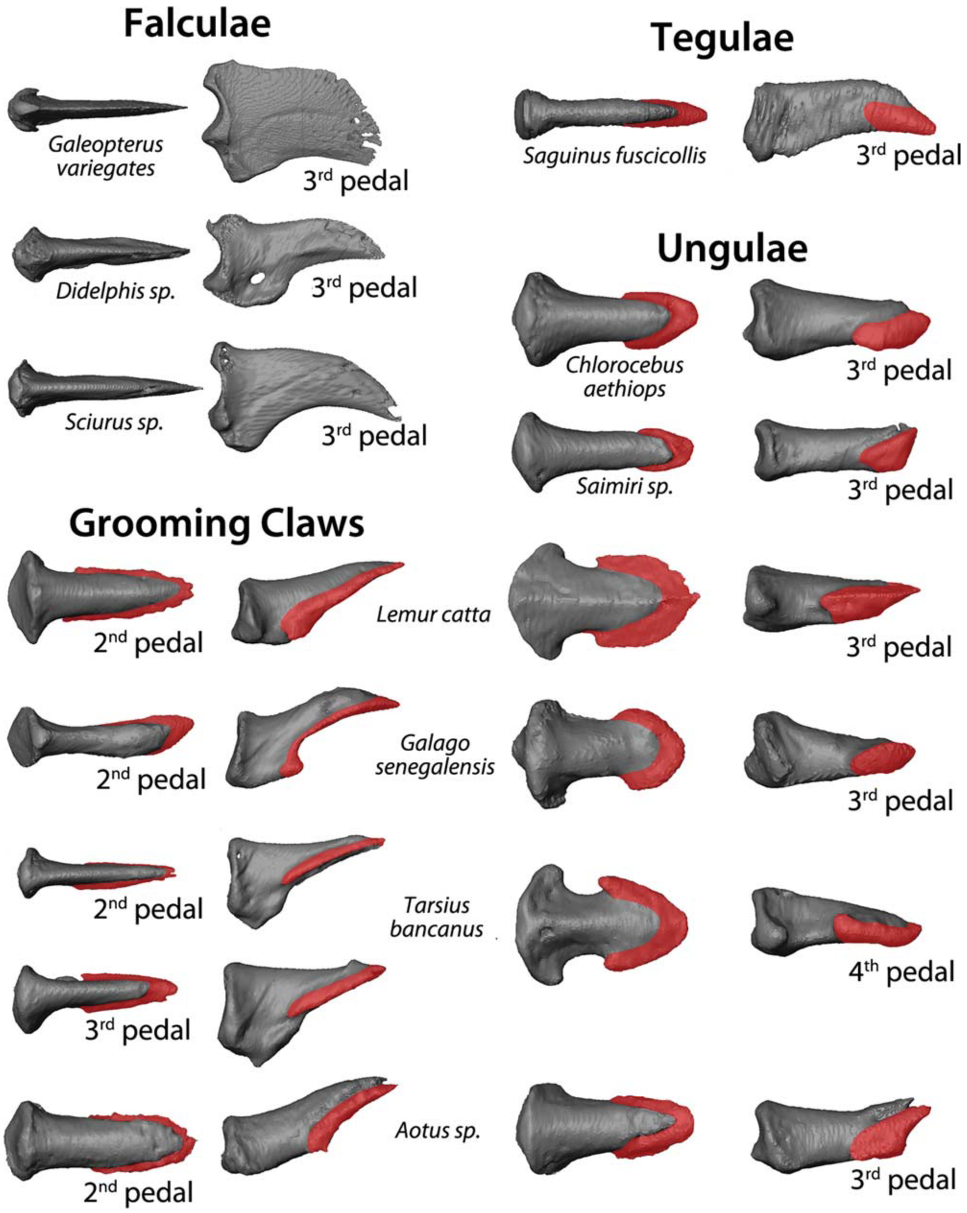

Fig. 9. Primate apical tufts. Apical tufts are highlighted in red, illustrating their presence on tegular and grooming phalanges. All digits have been scaled to a similar length.

falcular and tegular digits (Rosenberger, 1977; Garber, 1980). Specifically, it has been noted that the apical pads of falcular digits are less extensive and positioned ventral to the distal interphalangeal joint, while those of tegular digits are more extensive and positioned along the ventral surface of the shaft of the phalanx. The apical pads of tegular digits can certainly be observed to be more extensive than those of falcular digits (Fig. 5), though the precise position of the apical pad in falcular digits is variable. The apical pad of the pedal-grasping *Didelphis* does not overlap with the distal interphalangeal joint (Fig. 5: note that the proximal portion of the apical pad of *Tamandua* is absent due to the manner in which this digit was cut); but that of *Sciurus* does (Fig. 1A). Regardless, the most clear-cut difference between a tegular and falcular phalanx is the presence of an apical tuft in tegulars.

While tegular phalanges can be distinguished quantitatively from ungular phalanges in a multivariate context, the continuum between the two forms can be seen in the individual measures of shaft width and distal shaft height (Fig. 7). A great amount of variation is present within platyrrhine ungular phalanges in the form of height, width, the degree to which the shaft tapers, the proportion of bone which projects above and beyond the apical pad, and even the curvature of portions of the shaft (note the odd distal portion of the third pedal digit of *Aotus*) (Fig. 10). Therefore, it seems quite feasible that the form of an ungular phalanx could be modified into a tegular one through further increase in height

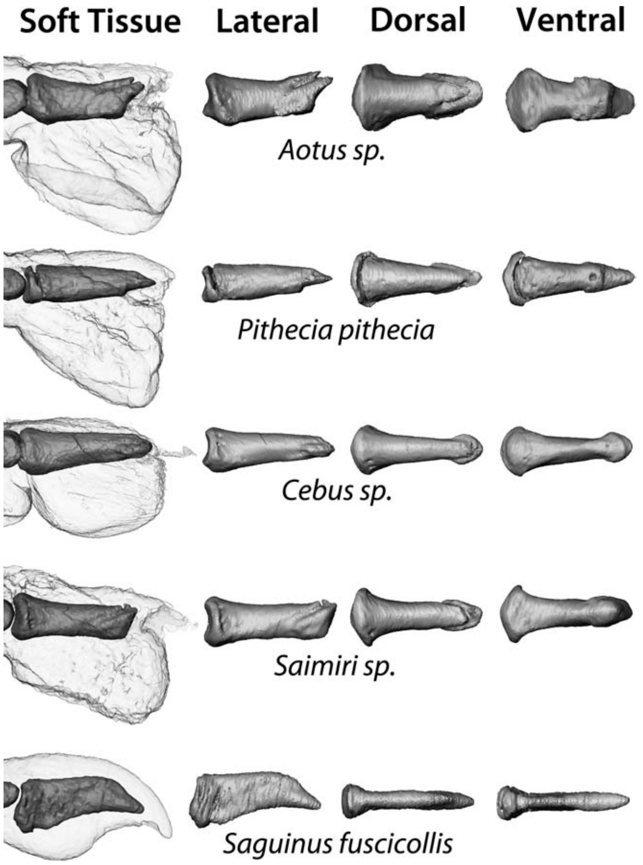

Fig. 10. Variation in platyrrhine third pedal digits. All digits have been scaled to a similar length.

and degree of distal tapering, a decrease in width, a proximal-ward repositioning of the apical pad, and a slightly increased curvature of the shaft (Hamrick, 1998). Further, it seems unlikely that if a falcular phalanx was modified into a tegular one, that a small but useless apical tuft would also be formed. This evidence strongly supports the position that tegulae are modified ungulae rather than falculae.

Grooming Claws

Grooming phalanges are clearly distinguished from other forms in this analysis. The distinguishing features of a grooming phalanx are a strong dorsal cant, a dorsoventrally shallow shaft and base, a shaft that projects far beyond the apical pad, and an apical tuft. These features (especially the apical tuft) suggest that grooming claws are not just simple retentions of an unmodified falculae. However, their does appear to be some variation among the grooming claws of different primate clades.

The Special Case of Tarsiers

The grooming phalanges of tarsiers are somewhat morphologically distinct. They appear to have a more flattened dorsal surface in lateral silhouette as opposed to the more contoured surface of strepsirhines (Fig. 9). They also have relatively mediolaterally narrower distal shafts and relatively dorsoventrally deeper proximal shafts when compared to those of strepsirhines. This indicates that the shaft of the tarsier grooming phalanx more strongly tapers in both width and height. There also appears to be higher variation in the extent of the apical tuft in tarsiers. In strepsirhines and platyrrhines, the apical tuft extends backward onto the volar process (Fig. 9). However, in both second and third pedal digits of *Tarsius bancanus* and the second pedal digit of *Tarsius spectrum* this tuft ends just distal to the process (Fig. 9), but the third pedal digit of *Tarsius spectrum* resembles the more extensive condition seen in strepsirhines and platyrrhines.

However, the most striking difference between tarsier and nontarsier primates is that tarsiers are unique in possessing a grooming claw on the third as well as on the second pedal digit. This condition may reflect a difference in function. Strepsirhines are described as using their grooming claws to scratch the fur around the head and neck (Hill, 1953; Jolly, 1967; Tenaza et al., 1969; Hutchins and Barash, 1976). Reports of strepsirhine grooming suggest that it is primarily done orally by licking and/or through the use of a tooth comb, while the grooming claw is used to scratch hard to reach areas (Tenaza et al., 1969; Hutchins and Barash, 1976). Unlike strepsirhines, tarsiers lack a dental comb. It may be that two narrow grooming claws used together may be capable of some degree of combing of the fur during scratching. Descriptions of tarsier self-grooming are limited, but they are reported to lick the fur and use grooming claws to scratch (Clark, 1924). When scratching, they hold the pedal digits flexed against the plantar surface of the foot, such that just the grooming claws are exposed (Clark, 1924). Additionally, nonprimate mammals are described as using a pair of grooming claws (the syndactylus second and third digits of diprotodonts) to comb the fur (Jones, 1921, 1925; Goodrich, 1935). However, it is not clear as to if or how this behavior might approximate that of tarsiers. Further, it is interesting to note that the exact pressures and scenarios that would result in a grooming claw in some mammals, but not others are poorly understood.

The Platyrrhine Grooming Claw

Grooming claws and grooming claw-like morphology has now been quantitatively demonstrated within platyrrhine monkeys. However, there is a great deal of variation among platyrrhine second pedal digits, particularly in dorsal cant. Most platyrrhines, and even two catarrhines in this sample, possess a second pedal distal phalanx that is more dorsally canted than the third (Fig. 8). Subsequent observations in *Brachyteles* and *Cebus* verify that the fourth and fifth digits are less canted than the second. It is possible that such a condition could represent intermediate stages in the acquisition or loss of grooming claws. However, a better understanding of within species variation is necessary to interpret this possibly intermediate condition. Among the platyrrhines in this analysis, *Aotus sp.* showed second pedal phalanges that clearly possess strepsirhine-like grooming claws (Fig. 11), while *Callicebus cupreus* possesses grooming claw-like morphology. Those of other ungulae-bearing platyrrhines may be dorsally canted, but are not differentiated from the third pedal digits in

Fig. 11. An owl monkey uses its foot to scratch the fur surrounding its head and neck. The grooming claw on its second pedal digit (top right) projects further dorsally than those of its other pedal digits (for example the third pedal digit illustrated below the second) which is likely an advantage for scratching through its thick pelage.

other ways. Most importantly, they lack a distal portion which projects far beyond the distal limits of the apical pad. Such structures are difficult to label as their functional significance is not clear and their morphology appears intermediate in form. However, they are considered here ungulae as they lack the characteristic shaft which projects beyond the apical pad. We also examined the second pedal digit of the callitrichine *Saguinus*, but it did not appear to differ much in cant nor other morphological features from the third. Unlike *Daubentonia*, callitrichines do not appear to possess grooming claws.

The Question of Grooming Claw Homology

The presence of a grooming claw on the third pedal digit only in tarsiers seems to be most easily explained by its independent origin within this lineage, but this does not necessarily apply to the second digit (Soligo and Müller, 1999). The grooming claws of tarsiers do appear to be different than those of strepsirhines, but it is not clear if these differences are enough to imply an independent origin of the second pedal grooming claws. Furthermore, it is unclear as to when the tarsier pattern of a third pedal grooming claw arose in primate evolution; the distribution of grooming claws in fossil tarsiiform and omomyiform euprimates remains undocumented.

The situation among platyrrhines is even more confusing. The phylogenetic relationships between *Aotus*, *Callicebus*, and other platyrrhine groups have been disputed. Analyses based on morphology place the two genera in the same clade as sakis and uakaris (Pitheciinae) while molecular analysis places *Callicebus* in the pitheiines and *Aotus* with callitrichines and cebines, the latter including *Cebus* and *Saimiri* (Schneider and Rosenberger, 1996; Wildman et al., 2009). It is thus interesting to note the unique presence of demonstrably distinct grooming claws in morphologically similar, yet genetically dissimilar, taxa (Fig. 12). If grooming claws are derived traits in platyrrhine primates and the genetic evidence for the phylogenetic positions of *Aotus* and *Callicebus* are accepted, convergent or parallel evolution in two lineages is implied. If morphological evidence is accepted and the two genera are united in a single clade, convergent or parallel evolution may still be implied by the dorsally canted phalanges present in both cebids (*Cebus* and *Saimiri*) and atelines (*Brachyteles*). On the other hand, if platyrrhine grooming claws are primitive retentions, the loss or reduction of grooming claws in various degrees is also implied along multiple platyrrhine lineages. At this point, there is no clear indication of the homology or polarity of this trait within platyrrhines.

Despite the possibility of convergent or parallel origins of grooming claws along three separate primate lineages, it seems most likely, given the commonality of a grooming claw and a range of grooming claw-like morphology on the second pedal digit, that the second pedal grooming claw is an ancestral trait for the group including strepsirhines, tarsiers, and anthropoids.

However, until the homologies and polarities of this trait complex are better understood, the absence or presence of a grooming claw should only be used with the utmost caution in considering the phylogenetic affinities of fossil primates. Clearly, a better understanding of the

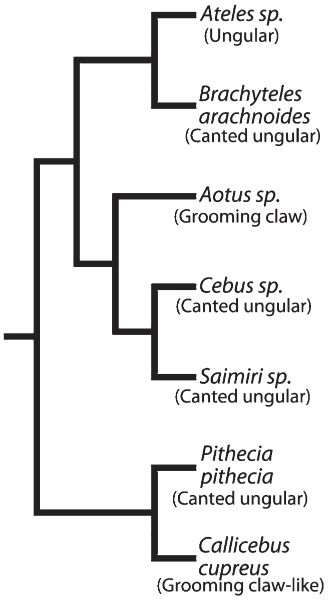

Fig. 12. The forms of platyrrhine second pedal distal phalanges and the phylogenetic relationships among species. Relationships are from molecular phylogeny of Wildman et al. (2009).

form and distribution of this structure among fossil primates is needed to better assess these questions.

Fossils

Turning to fossils, the presence or absence of grooming claws in extinct early euprimates is debated. For example, the second pedal digit of the adapid *Europolemur kelleri* is reported to bear a grooming claw (von Koenigswald, 1979; Franzen, 1994), but independent observations have not corroborated this (Dagosto, 1990; Williams et al., 2010). The absence of a grooming claw has been described in two other adapoid primates as well: the controversial *Darwinius masillae* and *Europolemur koenigswaldi* (Franzen et al., 2009). It is obvious that a clear and quantifiable definition of a grooming claw, as presented in this article, is required to unequivocally interpret the presence or absence of this feature in the fossil record. However, just what its presence or absence in adapoids might indicate is unclear. As previously addressed, its absence is unlikely to indicate phylogenetic affinities to anthropoids because grooming claws were likely to have been present in ancestral anthropoids. Assuming for a moment that lack of a grooming claw does, in fact, characterize basal anthropoids (and thus have been a product of convergent re-evolution in platyrrhines), the form of the second pedal digit needs to be determined for basal adapids, due to the possibility of parallel loss. Such a scenario would be consistent with evidence of other parallels between early adapid evolution and anthropoid evolution (e.g., Seiffert et al., 2009). *Cantius* is the oldest known adapiform and it retains the primitive euprimate dental formula of 2.1.4.3. It has undoubted close relationships with *Notharctus* and *Smilodectes*. Sampling any of these taxa would provide information much more applicable to the ancestral adapiform than data from middle Eocene European taxa. Clearly, our quantitative characterization of the grooming claw that has allowed its documentation in platyrrhines stands now to improve our view of primate evolution.

ACKNOWLEDGEMENTS

The authors thank S. Judex, S. Tommasini, and C. Rubin for providing access to HRxCT facilities at the Center for Biotechnology of the Department of Biomedical Engineering at Stony Brook University and to R. Secord of the University of Nebraska, D. Lunde and E. Westwig at the AMNH for access to specimens used in this analysis. The authors also thank William Jungers, Brigitte Demes, and John Fleagle for advice and suggestions on the development of this project. Finally, the authors also thank those who have provided support, assistance, and suggestions throughout this project: S. Blatch, J. Bunn, S. Carnation, K. Goodenberger, A. Gosselin-Ildari, H. Hassel-Finnegan, J. Herrera, A. Kingston, T. Nelson, G. Sorrentino, V. Venkataraman, and K. Viterbo.

LITERATURE CITED

Baden HP. 1970. The physical properties of nail. J Invest Dermatol 55:115–122.

Bloch JI, Boyer DM. 2007. New skeletons of Paleocene-Eocene plesiadapiforms: a diversity of arboreal positional behaviors in early primates. In: Ravosa MJ, Dagosto M, editors. Primate origins: adaptations and evolution. New York: Springer Science+Business Media, LLC.

Bluntschli H. 1929. Ein eigenartiges an Prosimierbefunde erinnerndes Nagelverhalten am Fuss von platyrrhinen Affen. Dev Genes Evol 118:1–10.

Bruhns F. 1910. Der nagel der halbaffen und affen ein beitrag zur phylogenie des menschichen nagels. Morph Jahr 40:501–609.

Cartmill M. 1972. Arboreal adaptations and the origin of the order Primates. In: Tuttle RH, editor. The functional and evolutionary biology of primates. Chicago: Aldine. p 97–122.

Cartmill M. 1974. Pads and claws in arboreal locomotion. In: Jenkins FA, Jr., editor. Primate locomotion. New York: Academic Press.

Clark WELG. 1924. Notes on the living tarsier (*Tarsius spectrum*). Proc Zool Soc Lond 94:217–223.

Clark WELG. 1936. The problem of the claw in primates. Proc Zool Soc Lond 106:1–24.

Dagosto M. 1990. Models for the origin of the anthropoid postcranium. J Hum Evol 19:121–139.

Fleagle JG. 1999. Primate Adaptation and Evolution, 2nd ed. New York: Academic Press.

Ford SM. 1980. Callitrichids as phyletic dwarfs, and the place of Callitrichidae in Platyrrhini. Primates 21:31–43.

Franzen JL. 1994. The Messel primates and anthropoid origins. In: Fleagle JG, Kay RF, editors. Anthropoid origins. New York: Plenum Press.

Franzen JL, Gingerich PD, Habersetzer J, Hurum JH, von Koenigswald W, Smith BH. 2009. Complete primate skeleton from the middle Eocene of Messel in Germany: morphology and paleobiology. PLoS ONE 4:e5723.

Garber PA. 1980. Locomotor behavior and feeding ecology of the Panamanian tamarin (*Saguinus oedipus geoffroyi*, Callitrichidae, Primates). Int J Primatol 1:185–201.

Godinot M, Beard KC. 1991. Fossil primate hands: a review and an evolutionary inquiry emphasizing early forms. Hum Evol 6:307–354.

Goodrich ES. 1935. Syndactyly in marsupials. Proc Zool Soc Lond 105:175–178.

Hammer Ø, Harper DAT, Ryan PD. 2001. Paleontological statistics software package for education and data analysis. Palaeontol Electron 4:9 pp.

Hamrick MW. 1998. Functional and adaptive significance of primate pads and claws: evidence from New World anthropoids. Am J Phys Anthropol 106:113–127.

Hamrick MW. 2001. Development and evolution of the mammalian limb: adaptive diversification of nails, hooves, and claws. Evol Dev 3:355–363.

Hamrick MW. 2003. Evolution and development of mammalian limb integumentary structures. J Exp Zool 298B:152–163.

Hershkovitz P. 1977. Living New World Monkeys (Platyrrhini), Vol. 1. Chicago: The University of Chicago Press.

Hildebrand M, Goslow G. 2001. Analysis of Vertebrate Structure, 5th ed. New York: Wiley.

Hill WCO. 1953. Primates Comparative Anatomy and Taxonomy I—Strepsirhini. New York: Interscience Publishers, Inc.

Hill WCO. 1960. Primates Comparative Anatomy and Taxonomy IV—Cebidae, Part A. New York: Interscience Publishers, Inc.

Homberger DG, Ham K, Ogunbakin T, Bonin JA, Hopkins BA, Osborn ML, Hossain I, Barnett HA, Matthews KL, II, Butler LG, Bragulla H. 2009. The structure of the cornified claw sheath in the domesticated cat (*Felis catus*): implications for the claw-shedding mechanism and the evolution of cornified digital end organs. J Anat 214:620–643.

Hutchins M, Barash DP. 1976. Grooming in primates: implications for its utilitarian function. Primates 17:145–150.

Jolly A. 1967. Lemur behavior: a Madagascar field study. Chicago: University of Chicago Press.

Jones FW. 1916. Arboreal man. New York: Longmans, Green and Co.

Jones FW. 1921. On the habits of *Trichosurus vulpecula*. J Mammal 2:187–193.

Jones FW. 1925. The hair pattern of a kangaroo; a study of cause and effect. J Mammal 6:13–17.

Jungers WL, Falsetti AB, Wall CE. 1995. Shape, relative size, and size-adjustments in morphometrics. Yearb Phys Anthropol 38:137–161.

Martin RD. 1992. Goeldi and the dwarfs: the evolutionary biology of the small New World monkeys. J Hum Evol 22:367–393.

Mittra ES, Smith HF, Lemelin P, Jungers WL. 2007. Comparative morphometrics of the primate apical tuft. Am J Phys Anthropol 134:449–459.

Panzer W. 1932. Beiträge zur biologischen anatomie des baumkletterns der säugetiere I. Das nagel-kralle-problem. Anat Embryol 98:147–198.

Pocock RI. 1917. The genera of the Hapalidae. Ann Mag Nat Hist 20:247–258.

Rosenberger AL. 1977. *Xenothrix* and ceboid phylogeny. J Hum Evol 6:461–481.

Rosenberger AL. 1979. Phylogeny, evolution and classification of New World monkeys. In. New York: City University of New York. p 603.

Schneider H, Rosenberger AL. 1996. Molecules, morphology, and platyrrhine systematics. In: Norconk MA, Rosenberger AL, Garber PA, editors. Adaptive radiations of neotropical primates. New York: Plenum Press.

Seiffert ER, Perry JMG, Simons EL, Boyer DM. 2009. Convergent evolution of anthropoid-like adaptations in Eocene adapiform primates. Nature 461:1118–1122.

Shrewsbury MM, Marzke MW, Linscheid RL, Reece SP. 2003. Comparative morphology of the pollical distal phalanx. Am J Phys Anthropol 121:30–47.

Soligo C. 1995. Anatomie und Funktion der Vorderextremität bein Fingertier (*Daubentonia madagascariensis*). In. Zürich: Zürich University.

Soligo C, Müller AE. 1999. Nails and claws in primate evolution. J Hum Evol 36:97–114.

Spearman RIC. 1985. Phylogeny of the nail. J Hum Evol 14:57–61.

Szalay FS, Dagosto M. 1980. Locomotor adaptations as reflected on the humerus of Paleogene primates. Folia primatol 34:1–45.

Tenaza R, Ross BA, Tanticharoenyos P, Berkson G. 1969. Individual behaviour and activity rhythms of captive slow lorises (*Nycticebus coucang*). Anim Behav 17:664–669.

Thorndike EE. 1968. A microscopic study of the marmoset claw and nail. Am J Phys Anthropol 28:247–262.

von Koenigswald W. 1979. Ein lemurenrest aus dem eozänen Ölschiefer der Grube Messel bei Darmstadt. Paläontol Z 53:63–76.

Wake MH, editor. 1992. Hyman's comparative vertebrate anatomy, 3rd ed. Chicago: The University of Chicago Press.

Weber M. 1928. Die Säugethiere. Jena: G. Fischer.

Wildman DE, Jameson NM, Opazo JC, Yi SV. 2009. A fully resolved genus level phylogeny of neotropical primates (Platyrrhini). Mol Phylogenet Evol 53:694–702.

Williams BA, Kay RF, Kirk EC, Ross CF. 2010. *Darwinius masillae* is a strepsirrhine—a reply to Franzen et al. (2009). J Hum Evol 59:567–573.

Zook EG. 2003. Anatomy and physiology of the perionychium. Clin Anat 16:1–8.